C. C. Karangelen
Lecturer,
Department of Mechanical Engineering,
The Catholic University of America,
Washington, DC 20064
Assoc. Mem. ASME

V. Wilczynski
Associate Professor,
The U.S. Coast Guard Academy,
New London, CT 06320-4192

M. J. Casarella
Professor,
Department of Mechanical Engineering,
The Catholic University of America,
Washington, DC 20064

Large Amplitude Wall Pressure Events Beneath a Turbulent Boundary Layer

Experimental data on the temporal records of the wall pressure fluctuations beneath a turbulent boundary layer have been acquired in a low-noise flow facility. The pressure data were first analyzed using long-time averaging techniques to determine the statistical properties and the results were compared to the baseline data of Schewe (1983). Next, the pressure records were conditionally sampled at various k threshold levels ($p'_w \geq k \cdot p_{rms}$) to detect large amplitude, positive and negative events which were then averaged and analyzed to determine their shape, duration, and frequency of occurrence. The intermittent large amplitude events are very short in duration, occur rather infrequently in time, but are a major contributor to the high frequency content of the wall pressure fluctuations. As an example, events where $p'_w \geq |3 \cdot p_{rms}|$ have an average duration of 14 viscous time units, occur 5 percent of the time and contribute 49 percent to the RMS value. The time between events appears to have a lognormal statistical distribution. The frequency of occurrence of the large amplitude events are consistent with the burst rate for flow structures and thus support the conjecture that the large amplitude events are associated with the near-wall bursting process.

Background

The wall pressure fluctuations beneath a turbulent boundary layer have received numerous experimental investigations and these have been reviewed by Willmarth (1975), Blake (1986), and Eckelmann (1990). Many of the earlier studies were concerned with obtaining quality data over a wide spectral range. Measurement errors due to transducer size and contamination by facility-related noise were major concerns in the high and low frequency regions, respectively. The recent investigation by Farabee and Casarella (1991) had overcome some of these problems. Data were obtained in a low-noise facility over a broad region of the spectrum and appropriate scaling laws for the low, mid, and high frequency ranges were established. It was concluded that flow structures in the inner and outer layers of the boundary layer contribute to the high and low frequency ranges of the spectrum, respectively. Because these data were obtained by unconditional averaging techniques, the contributions from intermittent organized events in the inner layer, sometimes referred to as the bursting process, were not distinctly observed in the spectrum of the wall pressure.

Several investigations have recently been made using conditional averaging techniques to examine the relationship between intermittent high amplitude wall-pressure peaks and flow structures in the near wall region. The most recent work is that of Haritonidis et al. (1990). Their results conclude that the wall pressure and flow structures in the buffer region are most prominently coupled through the normal component of velocity. No direct relationship between the wall pressure and isolated "*uv*" peak events was observed. Furthermore, by examining the weighted probability density $P(u, v)$ of u and v with the wall pressure, as well as the conditional averages of near-wall flow events and pressure peak events, they concluded that:

"Positive (peak) pressures are primarily associated with the fourth quadrant or sweep type events while negative (peak) pressures are associated with both the second and third quadrant or ejections and interactions inward, respectively."

"Quadrant," in the above quotation, refers to the u-v quadrant method developed by Lu and Willmarth (1973) for the statistical analysis of u-v stress events. It was also used in the Haritonidis study to detect isolated shear stress events. The quadrants are obtained by plotting the statistical data on a two axis graph, with u on the horizontal axis, v on the vertical axis. The result is a scatter plot which may be interpreted as a joint probability distribution, $p(u, v)$.

In Haritonidis et al. (1990), it was also stated that a one-to-one correspondence between pressure events and flow events does not exist. These findings contradict some earlier results of Johansson et al. (1987). It is apparent from these and other studies that the various coupling mechanisms between flow structures, in both the inner and outer layers of the boundary layer, and wall pressure fluctuations are quite complex.

The present research is an extension of the work of Farabee and Casarella (1991) by focusing on the use of conditional sampling techniques to analyze the data and investigate the

Contributed by the Fluids Engineering Division for publication in the JOURNAL OF FLUIDS ENGINEERING. Manuscript received by the Fluids Engineering Division May 22, 1992. Associate Technical Editor: D. M. Bushnell.

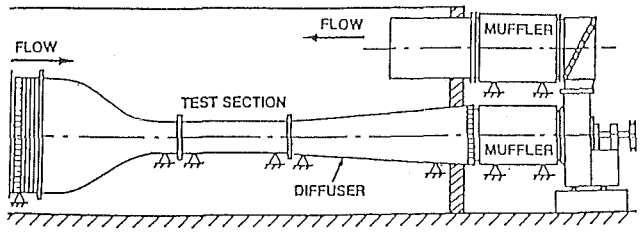

Fig. 1 The CUA wind tunnel facility

causality between flow structures and wall pressure events. As the first phase of this investigation, the authors obtained extensive data exclusively on the large amplitude positive and negative pressure events. The shapes, duration and frequency of occurrence of these events were computed (Karangelen, 1991) and these findings are detailed in this paper. Research now in progress (Wilczynski, 1991) consists of simultaneously measuring the (hot-wire) velocity at various locations across the boundary layer and the (pinhole microphone) wall pressure fluctuations.

Experimental Facility

A complete discussion of the facility, measurement techniques, and background noise can be found in Farabee and Casarella (1991) while a review of the data acquisition system and developed software is contained in Karangelen (1991). The following is a brief overview of the experimental facility.

Flow Facility and Measurement Techniques. The measurements were made in the wind tunnel at The Catholic University of America. The tunnel, illustrated in Fig. 1, has a 0.61 m square cross section with a 2.44 m long test section. Air is drawn through the tunnel by a low-speed centrifugal blower that is located downstream of the test section in an adjacent room. Acoustic mufflers are located upstream and downstream of the blower to minimize blower generated background noise. Exhaust air from the blower is circulated back into the room containing the tunnel allowing the air to be continuously recirculated. The inlet air first passes through a turbulence management section that consists of a honeycomb section and a series of screens of different mesh sizes. The contraction section was carefully designed to have a gradual static pressure distribution with no local separation on the wall. Boundary-layer trip wires are located on the test wall of the contraction section, upstream of the start of the test section, to ensure a fully developed turbulent boundary layer at the measurement locations. The wall pressure measurements were obtained at a location of approximately 1500 trip heights downstream of the trip wire. Tunnel free-stream velocity can be continuously varied from 6 to 30 m/s. Typical boundary-layer properties for the data to be presented are listed in Table 1.

Table 1 Summary of TBL characteristics

U_0 (m/s)	δ (cm)	δ^* (cm)	θ (cm)
15.5 (±0.1)	2.78 (±0.01)	0.45 (±0.01)	0.33 (±0.01)
28.3 (±0.1)	2.78 (±0.01)	0.43 (±0.01)	0.32 (±0.01)

u_τ/U_0	R_θ	d^+	δ^+
0.0403	3332	32.0	1169
0.0379	5929	56.6	2010

Wall pressure measurements were made on the smooth wall in the test section. To minimize spatial averaging effects, wall pressure fluctuations were measured with flush mounted 0.79 mm diameter pinhole microphones. The pinhole transducer consisted of a Bruel and Kjaer 0.3175 cm (1/8 in.) condenser microphone on which a blank cap, containing a 0.79 mm diameter hole ($33 \leq d \cdot u_\tau/\nu \leq 66$) was attached. The volume enclosed by the cap was kept small to ensure the Helmholtz resonance frequency of the cap system was above the frequency range of interest in the wall pressure measurements. A comparison calibration showed that the Helmholtz frequency occurs at approximately 25 Khz.

Special efforts were made during the measurements of the wall pressure to minimize the effects of both background noise and spurious free-stream turbulence levels. The spectral features of the free stream turbulence and the cross-spectra between free-stream velocities and wall pressure fluctuations were massed in order to assess the sources of noise contamination on the measurements (Helal et al., 1989). The data were found to be noise-free for frequencies above 70 Hz.

Data Acquisition Techniques. The data acquisition system (MASSCOMP 5450 Unix-based workstation) allowed pressure data to be simultaneously sampled, digitized, stored, and analyzed. In the experimental approach used to collect and analyze the wall pressure data, the power spectrum of the wall pressure signal are first examined using the dual channel FFT analyzer (HP 3562A) to determine the spectral features and the quality of the data. The temporal records of this pressure signal are then filtered to avoid aliasing, digitized, and stored on the hard disk. The data are also high pass filtered (f_{c0} = 70 Hz) to eliminate facility noise, and stored as a new record on the workstation's hard disk for post-processing.

The sampling rate was selected such that the time between sequential samples does not exceed one viscous time unit using the criteria:

$$f_{\text{sample}} > \frac{1}{t_\nu} = \frac{u_\tau^2}{\nu}.$$

At a free-stream velocity of 15.5 m/s, the data were sampled for 10 seconds at a 30 Khz sampling rate. This resulted in a time between samples of 0.8 viscous units. Data records were obtained over a range of flow speeds from 12 to 27 m/s.

Nomenclature

d = microphone diameter
d^+ = microphone diameter scaled on inner variables
f_{c0} = analog filter cutoff frequency
f_{sample} = digital sampling frequency
k = threshold value
$p(u, v)$ = joint probability distribution of u, v
p_{rms} = RMS pressure
p'_w = pressure fluctuation measured at the wall
q = dynamic head
RMS = root mean square
R_θ = Reynolds number based on momentum thickness
t = time
t^+ = time scaled on inner variables
$\langle t \rangle$ = average time, in units of t^+, between large amplitude events
Δt = average duration, in units of t^+, of large amplitude events
u = streamwise velocity component
u_τ = frictional velocity
U_0 = free-stream velocity
v = velocity component perpendicular to the wall
δ = boundary-layer thickness
δ^+ = boundary-layer thickness scaled on inner variables
δ^* = displacement thickness
θ = momentum thickness

Experimental Results

The wall pressure data were first examined using long-time averaging techniques to determine the statistical properties for comparison to the published data. Some of these results will be briefly reported in this paper. The data records were then conditionally sampled to detect large amplitude, positive and negative events. These events were averaged and analyzed to determine the characteristic shapes and the frequency of occurrence. These results will be presented in some detail.

Statistical Properties of Wall Pressure Fluctuations. The data to be presented will show that the probability distribution of amplitudes has features which are clearly different from a Gaussian signal. Specifically, in comparison to the Gaussian signal, the wall pressure fluctuations have more large negative and positive amplitudes. A comparison of the higher moments of the probability distribution between the present data and the Gaussian random signal illustrates the distinctions. The data exhibited a slight negative coefficient of skewness (-0.18, with a variance of .0025) with 0.0 for Gaussian data, and a larger coefficient of kurtosis (4.94, with a variance of .044) rather than 3.0 for the Gaussian signal. The negative skewness in the data indicates an asymmetry in the probability density distribution, with a slightly greater occurrence of negative amplitudes. The deviation in the kurtosis (flatness) value indicates that more large amplitude events are present. Also, it is expected that a signal with a high level of intermittency should have a high flatness value. In summary, the difference between Gaussian statistics and that seen by the measured data appears to be attributed to intermittent large amplitude pressure fluctuations, with a slight bias towards more negative events.

Schewe (1983) measured the probability distribution and its moments using transducers of various sizes. He demonstrated that the skewness and kurtosis values for increasingly large transducers approach that expected for a random Gaussian signal and concluded that measurements with large transducers lack the ability to discriminate the inherent features of the data. As more and more pressure producing events occur on the active face of a transducer, each can be considered an individual random process with its own probability density function. As the transducer size is increased, more pressure events are detectable simultaneously by the transducer. By virtue of the Central Limit Theorem, the statistics of the transducer output will approach Gaussian values with increasing transducer size.

The statistics of the present data were compared with the Schewe (1983) data to validate the quality of the data. Figure 2 compares the RMS value, skewness coefficient and kurtosis coefficient of the present data with Schewe's results for various dimensionless transducer sizes ($d^+ = d \cdot u_\tau/\nu$).

It is somewhat misleading to compare the statistical data from investigations at different Reynolds numbers in the form shown in Fig. 2 since it is difficult to separately account for both the effects of transducer size, which limits the high frequency resolution, and the variations of the wall pressure fluctuations with Reynolds number. This issue, as well as the scaling laws for the RMS values, are discussed in Farabee and Casarella (1991).

Skewness and kurtosis values from a direct numerical simulation of the pressure fluctuations in a turbulent channel flow were reported by Kim (1989). The d^+ for his simulation can be estimated from the streamwise grid spacing where $d^+ = \Delta x^+ = 17$. At the wall, the numerical simulation results obtained a skewness value of $-.10$ and a kurtosis value of 5.0. These values are consistent with those of Schewe and the present data.

Some warnings are in order regarding the interpretations of the statistical data. It should be noted that if the temporal record of the wall pressure contains both deterministic and random structures, a pronounced effect on the long-time statistics is expected (Alfredsson and Johansson, 1990). Furthermore, Sreenivasan (1991) states that intermittent (flow) structures cannot be described efficiently by the statistics of the distribution. He further states that for Gaussian data, the mean and variance describe the process completely; however, for highly intermittent structures, the first few moments give little clue as to their nature.

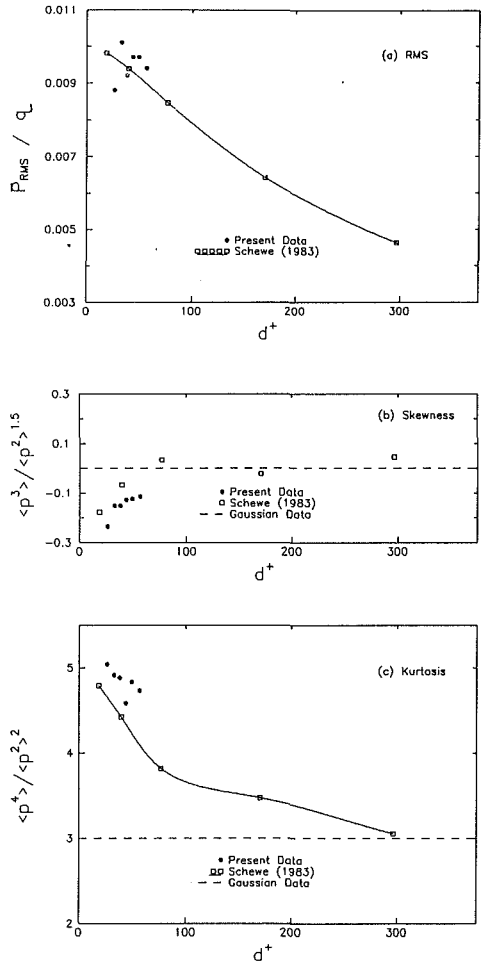

Fig. 2 Comparison of present data with the results of Schewe (1983). Experimental data have an error of approximately +/− 10 percent of magnitude.

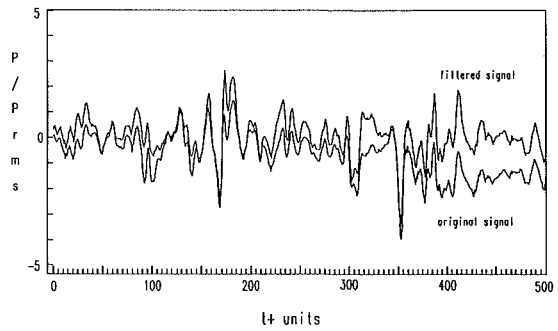

Fig. 3 Excerpt of a digital temporal record of the wall pressure signal at U_0 = 15.5 m/s. (Filtered signal has been bandpass filtered between 70 and 15,000 Hz)

Conditional Sampling of Large Amplitude Events. Visual inspection of the time records of the wall pressure revealed large amplitude events as seen in Fig. 3. A conditional sampling

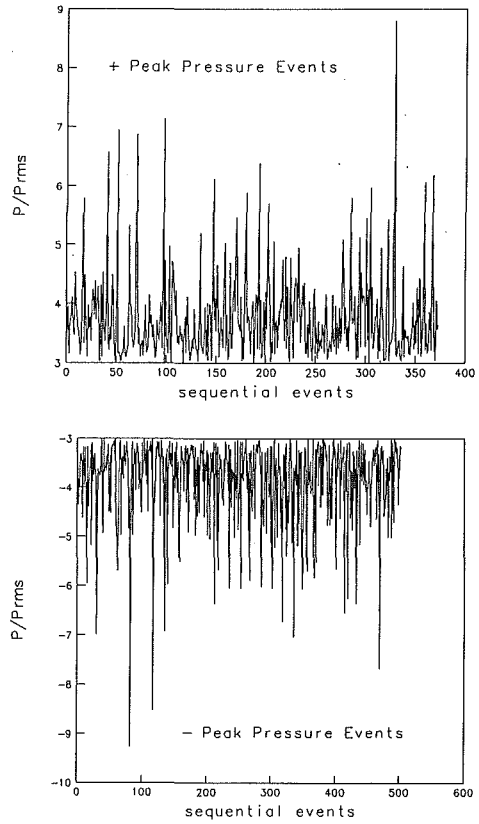

Fig. 4 Sequential large amplitude wall pressure events in excess of 3 RMS values for U_0 = 15.5 m/s: (*a*) positive events; (*b*) negative events

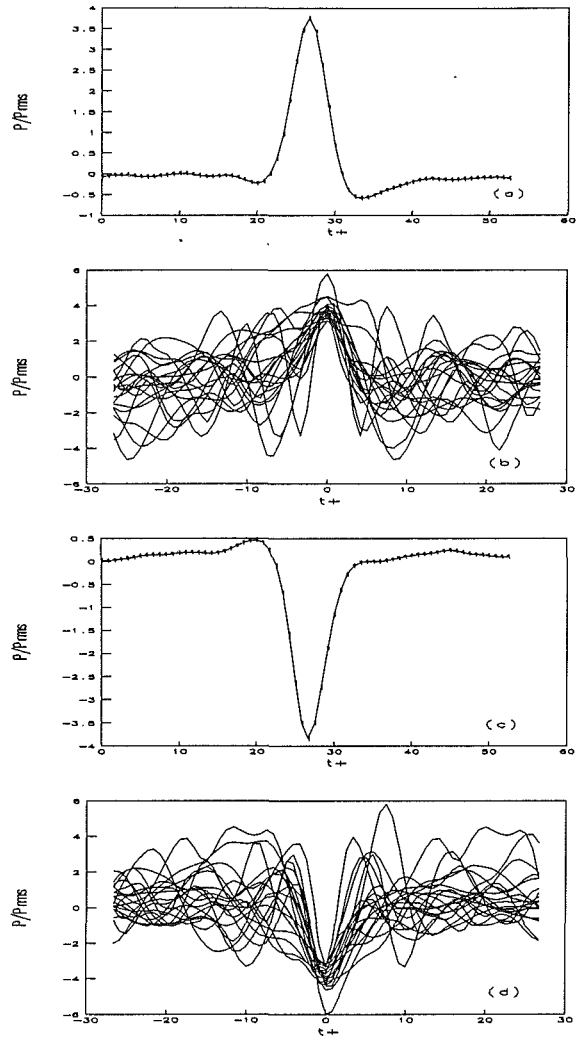

Fig. 5 Average and overlay of positive and negative large amplitude wall pressure events (k = 3.0; U_0 = 15.5 m/s)

approach to investigate the statistics of these pressure events was used. Peak pressure events were extracted from the contiguous time record if a measurement exceeded the threshold k, established by $p'_w \geq k \bullet p_{\text{rms}}$ for all positive peaks, and $p'_w \leq -k \bullet p_{\text{rms}}$ for all negative peaks. When the amplitude exceeded the threshold, an event was declared present. The time of occurrence of the event was colocated with the peak's maximum amplitude for positive events, and minimum amplitude for negative events. The duration of the event, Δt, was defined by the event's pre and post threshold zero crossings. It should be noted that many thresholds were investigated. The results to be presented are for a threshold k = 3 and these results show features that are typical of events using thresholds from 1 to 5.

Figures 4(*a*) and (*b*) are plots of peak positive and negative amplitudes, respectively, of events exceeding a threshold of k = 3 and displayed in sequential order of occurrence. The maximum positive pressure measured was 8.7 p_{rms} while the maximum negative pressure was $-9.2\ p_{\text{rms}}$. Figures 5(*a*) and (*c*) display the shape of events obtained by averaging the full ensemble of positive (or negative) events while Figs. 5(*b*) and (*d*) show an overlay of a subset of the individual events. Figures 6(*a*) through (*d*) are from the dame data records used in Fig. 5; however, these results were obtained by first normalizing each of the event's data points by their peak amplitude, then averaging the full ensemble of normalized events. From these results, it appears that the shape and duration of the events are independent of the event's amplitude since normalization had no noticeable effect on the averaged shape. In both cases, the positive and negative large amplitude events have clearly defined asymmetric wavelet shapes. These features are qualitatively similar to those obtained by Schewe (1983), Johansson et al. (1987), and Haritonidis et al. (1990).

The statistical properties of the events for various threshold values are presented in Table 2. The table lists the percentage of the total time and total RMS value that both positive and negative events contribute to the wall pressure fluctuations. The contributions were determined by computing the RMS values from all events that exceeded the current threshold. Consider, for example, the threshold k = 3. The data show that large amplitude events in excess of this threshold ($p'_w \geq 3 \bullet p_{\text{rms}}$) occur approximately 5 percent of the time and contribute to approximately 49 percent of the RMS value. These values (5 percent, 49 percent) are larger than that reported by Schewe (1 percent, 40 percent) and Johansson (6 percent, 18 percent). These differences are partially attributed to the methods used to estimate the contributions. Schewe's values were determined directly from higher moments of the probability density function. A comparison of the present results for k = 3 using this procedure show only 38 percent contribution to the RMS value compared to 49 percent contribution determined by considering the full event. Clearly, the probability distribution approach only takes into account that portion of the individual event that exceeds the threshold. The RMS calculations which incorporate the full event based on the axes crossings appear to be more realistic.

Frequency of Occurrence of Large Amplitude Events. An investigation of the time-dependent behavior of the wall pressure events was also pursued. This was done by determining

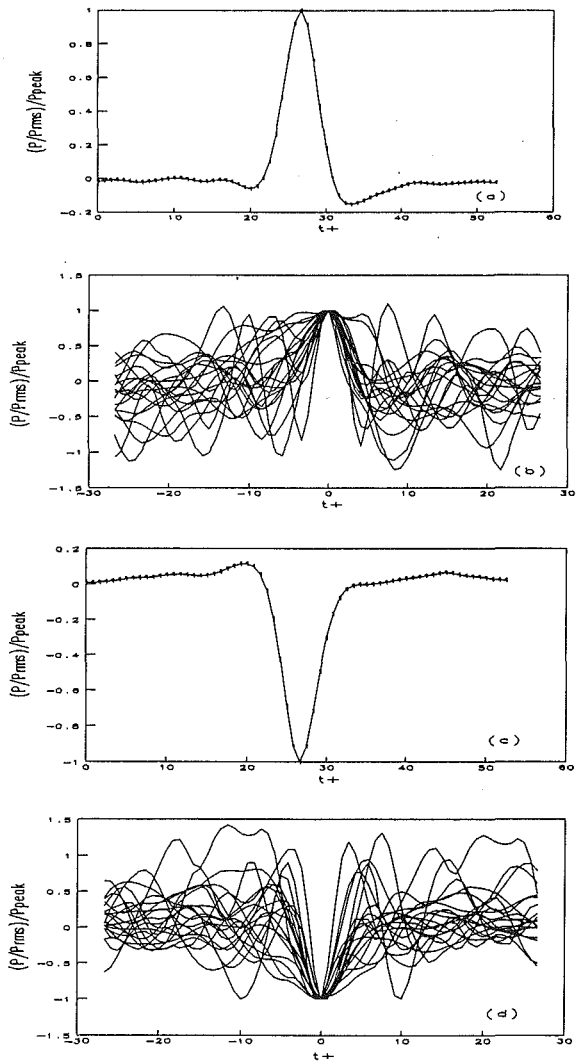

Fig. 6 Average and overlay of positive and negative large amplitude wall pressure events with normalized amplitudes (k = 3.0; U_0 = 15.5 m/s)

the statistical features of the duration of the events, and the time between events. The frequency of occurrence is defined as the reciprocal of the average time between events. For the purpose of this discussion, the 'time between events' is the time elapsed from the trigger point of one peak event to the next trigger point. The trigger point is defined as the time at which the signal exceeds the threshold condition. The time measurements are scaled on inner wall variables using the relationship

$$t^+ = \frac{tu_\tau^2}{\nu}.$$

The average duration of the events and the average "time between events" are tabulated in Table 3. This table contains separate information on both the positive and negative events. The average durations vary with threshold, but are approximately 10 to 16 viscous time units. There is negligible difference between the duration of the positive and negative events for calculations based on a large number of events. Schewe (1983) reported an average duration of 12 viscous time units. The present data are also consistent with the values obtained by Johansson et al. (1987).

As expected, the tabulated data show that the average value of the time between events increases with increasing values of the threshold for detecting events. For thresholds $k > 2$, the behavior appears to follow an exponential relationship as shown by the (approximate) linear fit using semi-logarithmic scaling

Table 2 Statistical properties of combined positive and negative large amplitude events. Mean values reported with standard deviations from the mean shown in parenthesis

k	%RMS	(err)	%Time	(err)
0.0	100.0	(----)	100.0	(----)
1.0	96.7	(0.13)	65.9	(0.63)
2.0	75.8	(0.37)	22.2	(0.36)
3.0	49.4	(0.80)	5.3	(0.16)
4.0	30.9	(1.41)	1.3	(0.12)
5.0	19.6	(1.78)	0.4	(0.06)
6.0	14.5	(0.92)	0.1	(0.03)

Table 3 Statistical properties of large amplitude events. Mean values reported with standard deviations from the mean show in parenthesis

(a) Positive large amplitude events

k	%Time	(err)	$\langle t \rangle$	(err)	Δt	(err)
0.0	50.87	(0.17)	20.66	(0.45)	10.10	(0.25)
1.0	33.57	(0.24)	48.02	(1.33)	15.56	(0.41)
2.0	10.47	(0.16)	164.9	(6.11)	16.54	(0.72)
3.0	2.15	(0.06)	724.5	(51.0)	14.58	(0.67)
4.0	0.47	(0.03)	2897.4	(280.7)	13.04	(0.92)
5.0	0.12	(0.02)	11454.	(3019.)	12.26	(0.79)

(b) Negative large amplitude events

k	%Time	(err)	$\langle t \rangle$	(err)	Δt	(err)
0.0	49.12	(0.17)	20.64	(0.44)	9.72	(0.22)
1.0	32.66	(0.24)	47.82	(1.77)	15.06	(0.48)
2.0	11.52	(0.24)	144.9	(6.53)	15.96	(0.79)
3.0	3.17	(0.16)	496.1	(31.6)	14.98	(1.33)
4.0	0.88	(0.07)	1640.0	(246.7)	13.64	(1.13)
5.0	0.26	(0.05)	4939.0	(938.9)	12.18	(1.45)

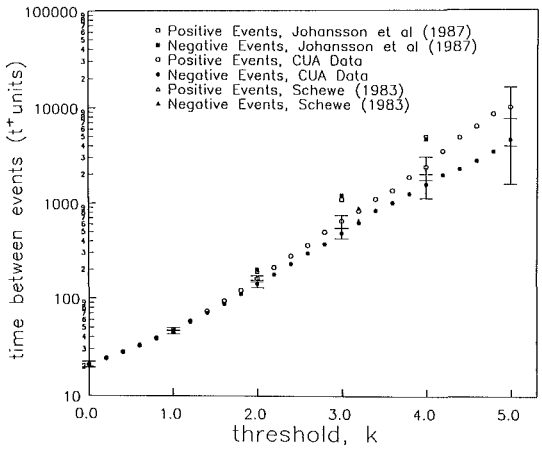

Fig. 7 The average time between large amplitude wall pressure events versus threshold for U_0 = 15.5 m/s. Error bars represent three standard deviations from the mean.

in Fig. 7. The values obtained by Johansson et al. (1987) for thresholds of 1, 2, 3, and 4 as well as Schewe (1983) for a threshold of 3.2 are also included in the Fig. 7. The limited data points of Schewe are in agreement with the present data while the Johansson data show some variations. As the threshold increases beyond k = 2, the average time between negative events is consistently less than the time between positive events. A corollary to this observation is that there are significantly more negative peaks than positive peaks over the same time record for peaks whose amplitudes exceeded k = 2.

The time between events for sequentially detected positive and negative events having a threshold of k = 3 are shown in Figs. 8(a) and (b). For this figure, events exceeding a threshold of k = 3 are sorted by sign into positive and negative

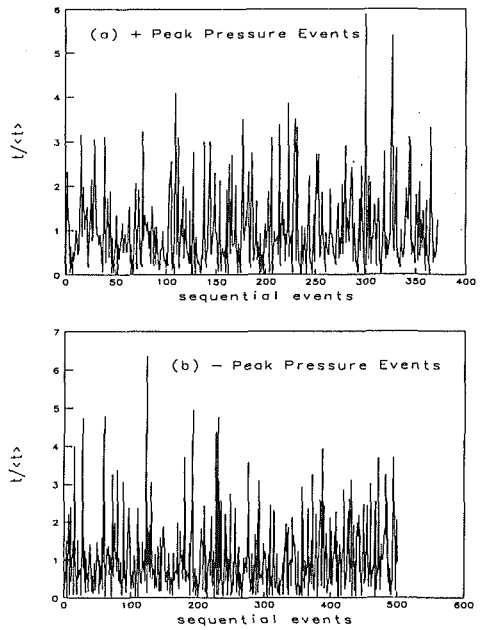

Fig. 8 Time between sequential events that exceed the 3 RMS value at U_0 = 15.5 m/s for: (*a*) positive events; (*b*) negative events

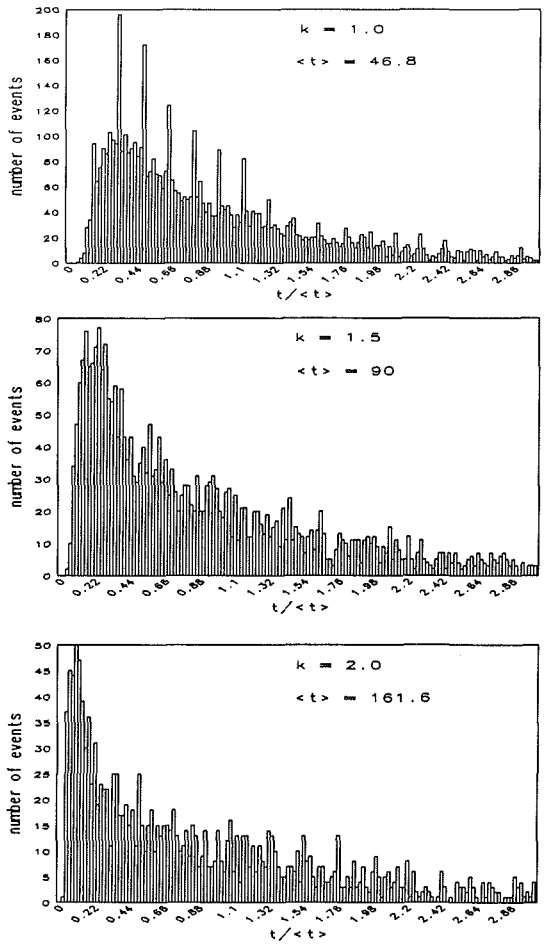

Fig. 9 Histogram of the distribution of time between positive large amplitude events at threshold values of 1.0, 1.5, and 2.0 for U_0 = 15.5 m/s

events and shown in their respective order of occurrence. As seen in the figures, there is no apparent order to the sequence of events. However, it does appear that several events below

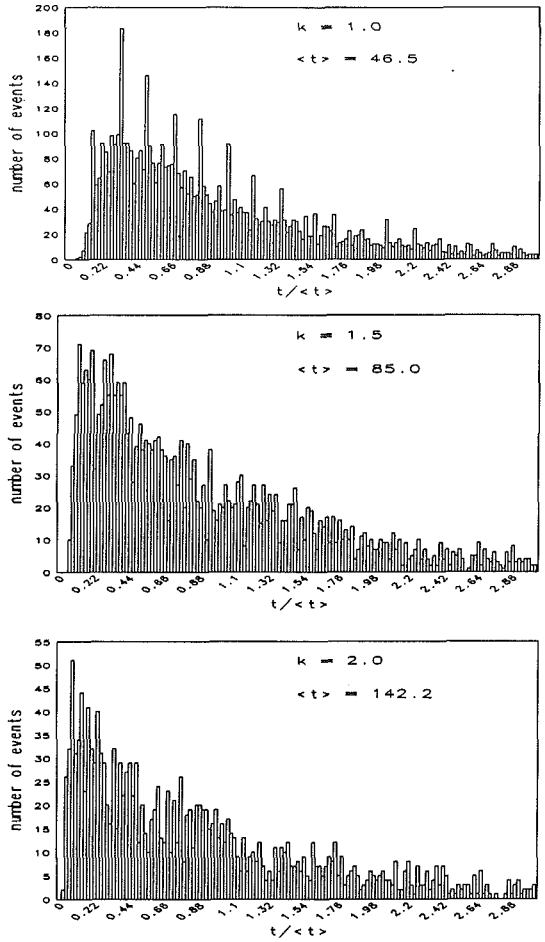

Fig. 10 Histogram of the distribution of time between negative large amplitude events at threshold values of 1.0, 1.5, and 2.0 at U_0 = 15.5 m/s

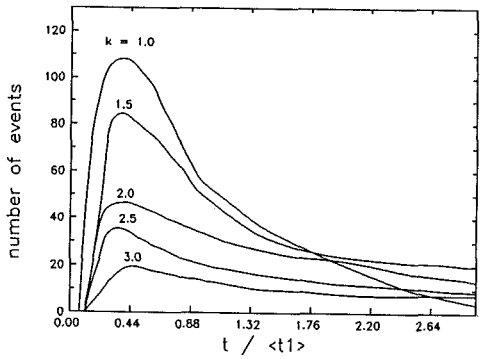

Fig. 11 Distribution of normalized time (re. $\langle t \rangle$ for the threshold k = 1) between negative peak pressure events for U_0 = 15.5 m/s

the average time occur prior to the occurrence of a long time delay between events. A preliminary examination of the relationship between positive and negative events revealed a pattern of 4 or 5 sequential negative events followed by a sequence of 3 or 4 positive events along the time record.

Histograms of the time between events for k = 1.0, 1.5, and 2.0 are shown in Figs. 9 and 10 for the positive and negative peaks, respectively. In each of the plots, the time between events has been normalized by the average value of time for that particular threshold. The results for higher values of k appear to follow the overall trend but were limited by the small sample size for the total number of events. Figure 11 is a

composite histogram of the time between events for the negative peaks over a range of threshold. In this figure, the time for each data set was normalized by the average time for the $k = 1$ threshold. To a first approximation, the distributions of time between events appear to follow a family of lognormal distributions (Karangelen, 1991).

A (Gaussian) white noise temporal record, which was bandpass filtered over the same frequency range as the real data, was analyzed and compared to the actual data shown in Fig. 9. As expected, the Gaussian results produced an equal number of positive and negative events with a classical lognormal distribution for the time between events for both positive and negative data sets. For the threshold of $k = 2$, the relative peak location and histogram shape appeared similar to the real data. The details can be found in Karangelen (1991).

Some Concluding Remarks

The goal of this investigation was to obtain noise-free wall pressure data in a quiet flow facility and to extend the database on the statistical features of wall pressure fluctuations. In the course of analyzing the extensive data, several significant observations have been made.

- — Digital samples of wall pressure fluctuations demonstrate non-gaussian statistics.
- — Large amplitude wall pressure events are major contributors to the RMS; 49 percent of the RMS value comes from events whose normalized peak pressures exceed a threshold of three times the RMS value and occur only 5 percent of the time.
- — Negative wall pressure events are seen to occur more frequently than positive events for all thresholds exceeding $k = 2$.
- — The probability distribution of time between events demonstrates quasi-lognormal behavior.

In this study, the focus of attention was to examine the large amplitude wall events in order to gain some new insight on the coupling between intermittent near wall flow structures and the wall pressure events. It had been proposed by Haritonidis et al. (1990) that the *negative pressure events* are associated with *outward ejections and inward interactions* of low speed fluid, while *positive pressure events* are associated with the *sweeps* of high-speed fluid toward the wall.

As previously discussed, there is some controversy regarding a one-to-one correspondence between "bursting events" and the large amplitude wall pressure events (Eckelmann, 1990; Haritonidis et al., 1990). This correspondence implies that for every ejection and/or sweep event that occurs locally in the near wall flow, there is a corresponding and exclusive large amplitude event seen in the pressure signatures at the wall. It futher implies that one can use the pressure signal received at the wall to trigger the detection of the burst events within the flow. This question was further addressed by Wilczynski (1992) and it is not possible to explicitly answer it with the present results. However, the secondary question, of whether the frequency of occurrence of wall pressure events (or average time between events) correlates with the occurrence of organized flow events, may shed some light on this issue.

For channel flows, Tiederman (1990) detected burst events using velocity measurements in the flow. He reported an average time between burst events of 90, scaled on inner variables, and this value was seen to be independent of Reynolds number. For boundary layer flows, the time between events is reported to be closer to 300 (Blackwelder and Haritonidis, 1983 and Willmarth and Sharma, 1984). By using these values as upper and lower bounds, the average time between events corresponds to a range between $2 \leq k \leq 3$ on Fig. 7 and thus is consistent with the occurrence of large amplitude wall pressure events.

Though the present results cannot resolve the basic issues regarding a one-to-one correspondence between bursting events and large amplitude wall pressure fluctuations, the analyses of the database on wall pressure events support the conjecture that there is a distinct relationship between intermittent events in the flow and large amplitude wall pressure events. This work has also provided a framework to pursue concurrent measurements of the velocity and wall pressure fluctuations in an effort to better understand the relationship between turbulent structures and wall pressure fluctuations. The recent data acquired by Wilczynski (1992) are now under extensive analyses to resolve these issues. Some of these findings were reported at the ASME winter meeting (NCA-Vol. 13, pgs. 165–80) and will be submitted for publication.

Acknowledgments

This research was sponsored by the Office of Naval Research under Contract No. N00014-88-K-0141 and grant No. N00014-91-J-1925.

References

Alfredsson, P. H., and Johansson, A. V., 1984, "Time Scales in Turbulent Channel Flow," *Physics of Fluids*, Vol. 27, pp. 1974–1981.

Blackwelder, R. F., and Haritonidis, J. H., 1983, "Scaling of the Bursting Frequency in Turbulent Boundary Layers," *Journal of Fluid Mechanics*, Vol. 132, p. 87–103.

Blake, W. K., 1986, *Mechanics of Flow-Induced Sound and Vibration*, Vol. II, Academic Press, New York, NY.

Bogard, D. G., and Tiederman, W. G., 1986, "Burst Detection with Single Point Velocity Measurements," *Journal of Fluid Mechanics*, Vol. 162, pp. 389–413.

Eckelmann, H., 1990, "A Review of Knowledge on Pressure Fluctuations," *Near Wall Turbulence*, S. J. Kline and N. H. Afgan, eds., Hemisphere Publishing Corporation, New York, NY, pp. 328–347.

Farabee, T. M., and Casarella, M. J., 1991, "Spectral Features of Wall Pressure Fluctuations Beneath Turbulent Boundary Layers," *Physics of Fluids A*, Vol. 3, No. 10, pp. 2410–2420.

Haritonidis, J. H., Gresko, L. S., and Breuer, K. S., 1990, "Wall Pressure Peaks and Waves," *Near Wall Turbulence*, S. J. Kline and N. H. Afgan, eds., Hemisphere Publishing Corporation, New York, NY, pp. 397–417.

Helal, H. M. S., Casarella, M. J., and Farabee, T. M., 1989, "An Application of Noise Cancellation Techniques to the Measurement of Wall Pressure Fluctuations in a Wind Tunnel," ASME Winter Annual Meeting, Report No. H00563 NCA 5, p. 49.

Johansson, A. V., Her, J., and Haritonidis, J. H., 1987, "On the Generation of High-Amplitude Wall Pressure Peaks in Turbulent Boundary Layers and Spots," *Journal of Fluid Mechanics*, Vol. 175, pp. 119–142.

Karangelen, C. C., 1991, "Temporal and Spectral Features of Wall Pressure Fluctuations Beneath a Turbulent Boundary Layer," Ph.D. dissertation, The Catholic University of America.

Kim, J., 1989, "On the Structure of Pressure Fluctuations in Simulated Turbulent Channel Flow," *Journal of Fluid Mechanics*, Vol. 205, pp. 421–451.

Lu, S. S., and Willmarth, W. W., 1973, "Measurements of the Structure of the Reynolds Stress in a Turbulent Boundary Layer," *Journal of Fluid Mechanics*, Vol. 60, p. 481.

Schewe, G., 1983, "On the Structure and Resolution of Wall-Pressure Fluctuations Associated with Turbulent Boundary-Layer Flow," *Journal of Fluid Mechanics*, Vol. 134, pp. 311–390.

Sreenivasan, K. R., 1991, "Fractals and Multifractals in Fluid Turbulence," *Annual Review of Fluid Mechanics*, Vol. 23, pp. 539–600.

Tiederman, W. G., 1990, "Eulerian Detection of Turbulent Bursts," *Near Wall Turbulence*, S. J. Kline and N. H. Afgan, eds., Hemisphere Publishing Corporation, New York, NY, pp. 874–887.

Wilczynski, V., 1991, "Correlation Between Organized Flow Structures and Large Amplitude Events Beneath a Turbulent Boundary Layer," presented at the 44th Annual Meeting of the American Physical Society.

Wilczynski, V., 1992, "Organized Turbulent Structures and Their Induced Wall Pressure Fluctuations," Ph.D. dissertation, The Catholic University of America.

Willmarth, W. W., 1975, "Pressure Fluctuations Beneath Turbulent Boundary Layers," *Annual Review of Fluid Mechanics*, Vol. 7, pp. 13–38.

Willmarth, W. W., and Sharma, L. K., 1984, "Study of Turbulent Structure with Hot Wires Smaller than the Viscous Length," *Journal of Fluid Mechanics*, Vol. 142, pp. 121–149.